Spontaneously Organized Molecular Assemblies. 3. Preparation and Properties of Solution Adsorbed Monolayers of Organic Disulfides on Gold Surfaces

Ralph G. Nuzzo,*† Florence A. Fusco,†,‡ and David L. Allara*⊥

Contribution from AT&T Bell Laboratories, Murray Hill, New Jersey 07974, and Bell Communications Research, Red Bank, New Jersey 07701. *Received July 18, 1986*

Abstract: This paper shows that stable, oriented, polyfunctional organic monolayers can be prepared by the spontaneous organization of structurally complex organic disulfides on polycrystalline gold substrates. Chemisorption proceeds to very high coverages, approaching that equivalent to the bulk-phase densities of the adsorbate molecules. The bonding to the surface is also highly specific, inasmuch as the chemisorption of the disulfide moiety is favored greatly over a wide range of other functionality. This latter feature allows the ready preparation of a broad variety of organic surfaces with well-defined microscopic and macroscopic characteristics. Several representative examples of monolayer films are described, their chemical and thermal properties explored, and their structures characterized by several techniques including infrared and photoelectron spectroscopies.

Interest in the properties of thin film organic materials, especially as regards organized mono- and multilayer structures prepared by Langmuir–Blodgett and self-assembly techniques, has grown enormously in recent years. The technological impetus for this rebirth—the relevance of such structures and materials to adhesion,[1] lubrication,[2] microelectronics,[3] photochemical[4] and electrochemical[5] processes, as well as biological interfaces[6] —has been discussed extensively and is now well appreciated. Equally important and, as yet, little discussed is the more basic contribution such studies might make to our understanding of the chemistry and physics of surfaces and interfaces in general. For example, to relate even a nominally simple macroscopic property such as wetting to a precise microscopic structure (or even to go in the opposite direction) is enormously difficult at present.[7] More involved interfacial properties and processes are characterized by a correspondingly increased level of complexity. As a consequence, progress in these areas will require interdisciplinary approaches involving the development and integration of such specialties as theory, synthesis, and materials characterization especially as they relate to surfaces and interfaces.

In this current paper we describe our results on the chemisorption of organic disulfides on elemental gold surfaces[8] and detail the application of reflection infrared and X-ray photoelectron spectroscopies, as well as ellipsometry and physical property measurements to the study of structure, reactivity, and surface bonding in this chemisorption system. Further, we detail a seemingly useful and general application of this class of chemisorption reaction, namely, the orientation of polar organic functionality at an ambient interface via self-assembly. The utility of these unusual monolayer structures to serve as substrates in more elaborate physical studies is demonstrated with representative examples.

Experimental Section

Sample Preparation and Treatment. Samples for the majority of the experiments performed were made by the vapor deposition of gold (both >99.999% and 99.99% purity materials) from resistively heated tungsten boats onto clean silicon single crystals which had been polished to high optical quality (see below). The substrate temperature was near but slightly above ambient temperature during the deposition. All depositions were made in a modified Varian evaporator equipped with a cyro-pump and operating with a base pressure of $\sim 1 \times 10^{-8}$ torr. Film thicknesses were measured with a quartz crystal thickness monitor. Typical mass coverages of ~2000 Å of gold were used. For most experiments strong adhesion of the gold film to the single crystal substrate was required. To promote adhesion, a preflash of ~150 Å of chromium was used. After the deposition, the chamber was backfilled with research purity N_2; the samples were removed and subjected to chemical treatment or spectroscopic examination with minimal delay. Most experimental results were quite reproducible with longer delay times up to the point of several days for samples in closed containers or several hours for samples exposed to the laboratory ambient. We did observe a significant tendency for the samples to become irreversibly contaminated under these latter conditions, however, and, as such, it is not recommended.

Solution treatments normally consisted of the direct immersion of the gold substrates into solutions (concentrations in the range 0.01 to 0.001 M) of the given disulfide in an appropriate high-purity solvent at ambient temperature. Immersion times were varied from several minutes to several days; in general, immersion times of several hours appeared to give results comparable to those obtained with longer incubations for most of the absorbates examined. We note that adventitious contaminants on the gold substrates may negate these observations. After immersion, the samples were rinsed with solvent and spun dry on a Headway photoresist spinner. Fresh disulfide solutions were made regularly as these materials appeared to be reasonably sensitive to decomposition (oxidation) in dilute solution. Additionally, best results were always obtained using polypropylene or Teflon containers rather than glass for the incubations.

Infrared Measurements. IR spectra of adsorbates were taken by reflection of the incident beam at an angle of incidence of 86° (4° off glancing) using p-polarized radiation. A nitrogen-purged Digilab 15-B Fourier transform spectrometer was used in conjunction with modified optics, which permit focusing of the beam outside the instrument, and equipped with stops and apertures to give an $\sim f/15$ beam focusing to an ~3-mm spot. A liquid-nitrogen-cooled mercury–cadmium–telluride (MCT) detector, operated in the photovoltaic mode, was used. Spectra were taken at 2-cm^{-1} resolution with a mirror speed of 1.4 cm/s. The interferograms were collected in double precision and Fourier transformed using triangular apodization. Typically, 800 scans were averaged to yield spectra with acceptable signal-to-noise ratios. Reference spectra were obtained on freshly evaporated gold mirrors. The procedures used to check and clean these reference substrates, when necessary, have been described previously.[9]

Spectra of bulk compounds dispersed in KBr were obtained in transmission at normal incidence. All such samples were prepared and manipulated under an atmosphere of dry, research purity nitrogen.

† Bell Laboratories.
‡ Current Address: Department of Material Science and Engineering, Massachusetts Institute of Technology, Cambridge, MA 02139.
⊥ Bell Communications Research.

(1) Kaelble, D. H. *Physical Chemistry of Adhesion*; Wiley-Interscience: New York, 1971, and references cited therein.
(2) Bowden, F. P.; Tabor, D. *The Friction and Lubrication of Solids*; Oxford University Press: London, 1968, and references cited therein.
(3) Roberts, G. G. *Adv. Phys.* **1985**, *34*, 475–512.
(4) Whitten, D. G. *Angew. Chem., Int. Ed. Engl.* **1979**, *18*, 440–450.
(5) See, for example: Faulkner, L. R. *Chem. Eng. News* **1984**, 28–45. Murray, R. W. In *Electroanalytical Chemistry*; Bard, A. J., Ed.; Marcel Dekker: New York, 1984; Vol. 13 and references cited therein.
(6) See, for example: Waldbillig, R. C.; Robertson, J. D.; McIntosh, T. J. *Biochim. Biophys. Acta* **1976**, *448*, 1–14, 15–28. Kornberg, R. D.; McConnell, H. M. *Biochemistry* **1971**, *10*, 1111–1118 and references cited therein.
(7) Holmes-Farley, S. R.; Reamey, R. H.; McCarthy, T. J.; Deutch, J.; Whitesides, G. M. *Langmuir* **1985**, *1*, 725–740. Schwartz, L. W.; Garoff, S. *Ibid.* **1985**, *1*, 219–230.
(8) Nuzzo, R. G.; Allara, D. L. *J. Am. Chem. Soc.* **1983**, *105*, 4481–4483.
(9) Allara, D. L.; Nuzzo, R. G. *Langmuir* **1985**, *1*, 52–66.

0002-7863/87/1509-2358$01.50/0 © 1987 American Chemical Society

Reflection infrared measurements made at higher temperatures were carried out by mounting samples, prepared as described above except using quartz as the initial substrate, on a copper support block. The assembly was resistively heated using a nichrome wire strip heater placed against the back of the copper block. The temperature was monitored with a thermocouple placed in a hole in the side of the quartz substrate and controlled to ±1 °C using a Leeds-Northrup temperature controller.

X-ray Photoelectron Spectroscopy. A modified Kratos XSAM 800 photoemission spectrometer utilizing a hemispherical analyzer and operating in a fixed analyzer transmission mode was employed for data acquisition. The instrumental resolution was ~1.1 eV, using a 2-mm mechanical aperture in conjunction with a Mg Kα X-ray source. Digital data were acquired by using 0.05-V steps. The base operating pressure was $<5 \times 10^{-11}$ torr.

Ellipsometry Measurements. Ellipsometric measurements were made using a Rudolf 423 null ellipsometer equipped with a Babinet-Solet compensator set for $\pi/4$ retardation and with the optical axis at 45° to the instrument vertical axis. Using a 70° angle of incidence at the sample, measurements were made with an ~1-mm diameter beam at 623.8 nm (He–Ne laser). Additional measurements were also made using 442.0-nm radiation (He–Cd laser). Such measurements showed little difference (within the limits of spot-to-spot variations and the experimental error limit of ca. ±1.0 Å) in the thicknesses calculated using these two sources; for convenience, most were made using the 623.8-nm radiation of the H–Ne laser.

Radioisotopic Labeling. Site densities of disulfide derivatized gold surfaces were determined using an acetylated derivative of *trans-o*-dithiane-4,5-diol (DTT-H). This material was prepared via the extended incubation of the anhydrous disulfide with a slight excess of 2 equiv of tritiated acetic anhydride (specific activity = 49.8 mCi/mmol, NEN) in distilled, anhydrous chloroform. Gold mirror samples evaporated on Teflon were used in these experiments. The solid was counted directly, after extensive washing in $CHCl_3$ and toluene, in Aquasol-2 scintillation cocktail (NEN) using a Beckman 300 scintillation counter. Results are corrected for a 1-π counting geometry.

Electron Microscopy. Scanning electron micrographs (SEM) were obtained directly on the gold substrates, using a JEOL CX-100 STEM, while TEM data were obtained using a JEOL 2000FX TEM. TEM samples were configured for cross-sectional analysis. These were prepared by the standard technique of ion milling on a thin cross-section slice of the gold and chromium covered silicon substrates.

Sources and Preparation of Compounds. DTT-H and dithiodipropionic acid were obtained from Aldrich and recrystallized once before use. Cystamine hydrochloride was obtained from Sigma and was converted to the free base by treatment with a stoichiometric quantity of sodium methoxide in diethyl ether at ~0 °C. Dimethyl disulfide and di-*n*-butyl disulfide were obtained from Aldrich and distilled prior to use. The remaining linear aliphatic disulfides were prepared from the corresponding thiols (Aldrich) by oxidation with aqueous hydrogen peroxide according to procedures described in the literature.[10] *Caution*: these reaction mixtures failed to show a positive indication of excess peroxide using iodide–starch test paper. Diundecanoic acid 11,12-disulfide was a gift of Professor George M. Whitesides. The bisacylated derivatives of dithiothreitol were prepared according to minor modifications of literature procedures[11] using a slight excess of twofold equivalents of the appropriate acid chloride except for the case of the trifluoroacetate derivative where trifluoroacetic anhydride was used. Reactions were carried out either in diethyl ether or methylene chloride solution at ~0 °C using a twofold excess of pyridine as a base. The isolated products were purified by repeated (2×) recrystallization. The materials obtained were characterized by IR, ^{1}H NMR, and elemental analysis. A persistent fatty acid impurity was noted in the hexadecanoate ester derivative but was easily removed, prior to chemisorption studies, by scrubbing a fresh, adsorbate-containing solution with high-purity, basic alumina.

Results

Film Thicknesses from Ellipsometry Data. Film thicknesses were calculated from ellipsometry data which were obtained and analyzed by procedures which have been described previously.[12] Untreated gold substrates (see above) were measured quickly (within several minutes) after removal from the evaporator. Pseudo-dielectric functions calculated from these values served to characterize the "clean" substrate. The samples were immersed directly into solutions of the disulfide (10^{-2}–10^{-3} M) in an appropriate solvent. Immersion times of 15 min to several hours were typically used. These samples then were removed from the solution, rinsed with fresh solvent, spun dry, and remeasured; thicknesses were calculated as described previously. The values obtained for the adsorbates listed in Table I are given in Figure 1 which plots the measured film thickness against the theoretical value which would characterize a closest packed monolayer of maximum adsorbate extension. It was noticed in many instances that longer immersion times did result in the formation of "thicker" overlayers. Although this effect was not examined in detail (it qualitatively appeared to be of the order of ~5 to 10% of the initial film thickness), it was observed that the appearance and rate of thickening processes were erratic. That they are seen at all originates in part, we believe, from contamination of the substrate by materials in the laboratory ambient. In the data in Figure 1, a value for the refractive index of $n = 1.50$ was used except where better values were available. Errors in assigning appropriate values of n fall within a range of $\Delta n = 0.05$. This corresponds to an ~1.5–2-Å thickness range. Even with this uncertainty, which exists for only a few compounds, the correlation demonstrated in Figure 1 remains quite useful.

As mentioned above, Figure 1 uses values of estimated upper limits of film thickness which we obtain from assemblies of close-packed, space-filling, molecular models. For these estimates we assume for simplicity that an unbroken S–S bond is coplanar to the surface and that the molecule adopts a conformation, consistent with unstrained closest packing, that maximizes its extension along the surface normal. Values for a configuration

Table I. Compilation of Organic Disulfides Used in Chemisorption Studies on Polycrystalline Gold Substrates

molecule	abbreviation	symbol in Figure 1
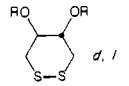		
R = H	DTT-H	○
R = $CF_3(CF_2)_6CO$	DTT-F_p	⊗
R = $CH_3(CH_2)_{14}CO$	DTT-hexadecanoate	◒
R = $(p\text{-}NO_2)C_6H_4CO$	DTT-PNBA	◓
R = CH_3CO	DTT-OAc	●
R = CF_3CO	DTT-TFA	⊙
$(HO_2C(CH_2)_2S)_2$		□
$(HO_2C(CH_2)_{10}S)_2$		■
$(H_2N(CH_2)_2S)_2$		▽
$(CH_3(CH_2)_{17}S)_2$		
$(CH_3(CH_2)_{15}S)_2$	HDDS	▲
$(CH_3S)_2$		
$(CH_3(CH_2)_3S)_2$		
$(CH_3(CH_2)_7S)_2$		
$(CH_3(CH_2)_9S)_2$		
$(CH_2CH(CH_2)_{20}S)_2$		◇

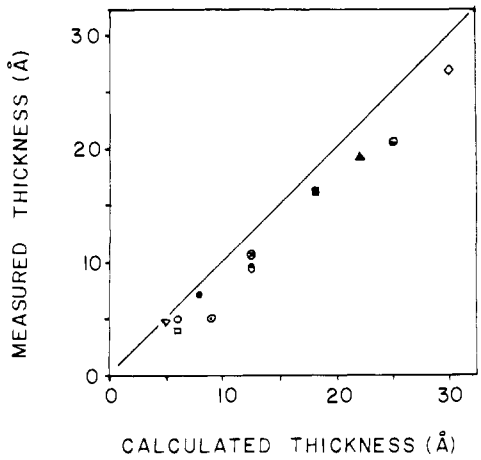

Figure 1. A plot of measured film thicknesses determined by ellipsometry vs. that determined from space-filling models for adsorbates exhibiting a closest packed arrangement oriented along the surface normal.

(10) McAllan, D. T.; Cullum, T. V.; Dean, R. A.; Fidler, F. A. *J. Am. Chem. Soc.* **1951**, *73*, 3627–3631.
(11) Field, L.; Khim, Y. H. *J. Org. Chem.* **1972**, *37*, 2710–2714.
(12) Allara, D. L.; Nuzzo, R. G. *Langmuir* **1985**, *1*, 45–52.

Table II. Mode Assignments and Calculated Transition Moment Orientations for $(C_{16}H_{35}S)_2$ Monolayers

frequency, cm^{-1} obsd	frequency, cm^{-1} calcd	assigned mode[a]	$I_{obsd}/3I_{calcd}$	ϕ_{mz},[e] deg
2965	~2961	CH_3 asym, str, r_a^-	0.67–1.0	0–35
~2953, 2958	~2943, 2950, 2955	CH_3 asym str, r_b^-	0–0.33	55–90
2938	2930[b]	CH_3 sym str,[d] r^+ (FR)	0.33–1.0	0–55
2918	2920	CH_2 asym str, d^-	0.25[c]	60
2893	~2893	CH_2 sym str,[d] d^+ (FR)	0.25–0.56	42–60
2878	2872	CH_3 sym str, r^+	0.78–1.0	0–28
2850	2850	CH_2 sym str, d^+	0.123	70

[a] Mode nomenclature taken from: Snyder, R. G.; Hsu, S. L.; Krimm, S. *Spectrochim. Acta, Part A* **1978**, *34*, 395–406. [b] Not resolved, frequency taken from reference in footnote *a*. [c] Corrected for line-width difference. [d] Due to Fermi resonance; see above reference and Hill, I. R.; Levin, I. W. *J. Chem. Phys.* **1979**, *70*, 842–851. [e] Angle between surface normal and mode transition dipole moment; see text.

Table III. Mode Assignments and Calculated Transition Moment Orientations for DTT-Hexadecanoate Monolayers

frequency, cm^{-1} obsd	frequency, cm^{-1} calcd	assigned mode[a]	$I_{obsd}/3I_{calcd}$	ϕ_{mz}, deg
2968	(2)	CH_3 asym str, r_a^-	~1	~0
2958	2957	CH_3 asym str, r_b^-	0.20–0.33	53–63
2924	2918	CH_2 asym str, d^-	0.43[c]	49
2880	2874	CH_3 sym str, r^+	0.56–1.0	0–42
2853	2851	CH_2 sym str, d^+	0.40[c]	51
1735	1736, 1727 (sh)	C=O str	0.14	68
1469	1471	CH_2 scissors def	~0.08	~73
1409	1417			
1384	1385			
1277, 1293	1277, 1287			
1267	1257, 1265	cc chain		
1246	1239, 1245	wag–twist		
1224	1225	progression		
1188, 1198	1198, 1205			
1174	1175	C–O str	0.77	~29
1117	1099			

[a] See footnotes *a* and *d*, Table II. [b] Not resolved in the spectrum. [c] Corrected for line-width difference.

with a dissociated S–S bond are nearly identical. Even given these extreme assumptions, the data in the figure clearly show that a broad correlation of structure/coverage exists over a wide range of adsorbate molecular structure.

In Figure 2, we present complementary ellipsometry data obtained for a homologous series of adsorbates, the di-*n*-alkyl disulfides. Although the data show some scatter, reflecting in part the difficulty in obtaining true (i.e., noncontaminated) substrate dielectric constants, it demonstrates a correlated pattern of film growth from the smallest (CH_3SSCH_3) to largest ($(CH_3(CH_2)_{17}S)_2$) disulfides examined. The slope is very close to what one expects from a series in which the chain length is sequentially increased by one methylene group.

Infrared Spectra. Infrared reflection spectra of films on gold were obtained for a number of different disulfides. Selected examples are shown in Figures 3–5 for hexadecyl disulfide (HDDS) and the hexadecanoate and *p*-nitrobenzoate (PNB) derivatives of DTT–H. These films are representative of a variety of molecular structures we have examined and illustrate the general capability to generate useful spectra for such materials. These

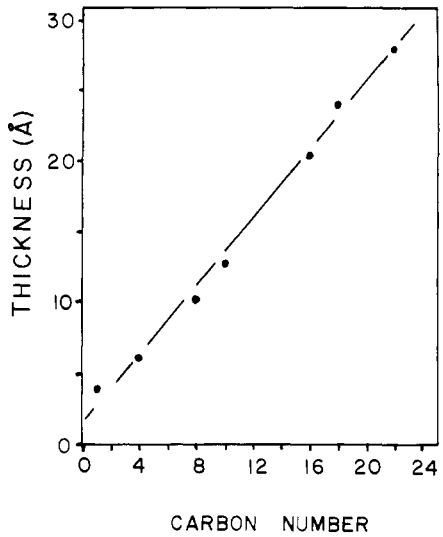

Figure 2. A plot of measured film thicknesses determined by ellipsometry vs. the number of carbon atoms in a single alkyl chain in a homologous series of di-*n*-alkyl disulfides. In each case, an $\sim 1 \times 10^{-2}$ M solution of the disulfide in *n*-hexadecane was used to prepare the adsorbate film. Three-day immersion times were also used throughout the series.

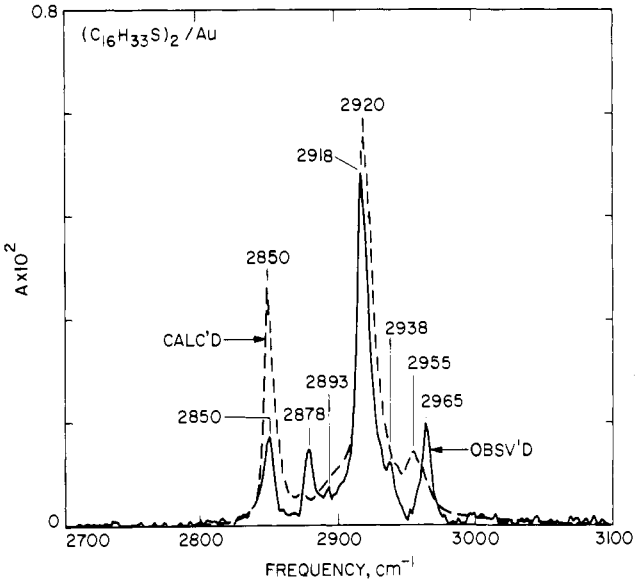

Figure 3. Infrared spectra for $(n\text{-}C_{16}H_{33}S)_2$ in the high-frequency region (see text): (---) calculated reflection spectrum; (—) observed spectrum. Methods used to obtain calculated spectra are described in the text.

Table IV. Mode Assignments[a] and Calculated Transition Moment Orientations for DTT–PNB Monolayers

frequency, cm^{-1} obsd	frequency, cm^{-1} calcd	assigned mode	$I_{obsd}/3I_{calcd}$	ϕ_{mz}, deg
1736	1748, 1734	C=O str	0.149	67
1609	1608	Ar cc str, 8a (A_1)	0.548	42
1539	1530	NO_2 asym str	0.250	60
	1412			
1352	1350	NO_2 sym str	0.376	52
1325	1326	Ar cc str, 14 (B_2)	0.583	40
1279	1282	C–O str	0.492	45
1123	1122	Ar CH bend ip 18b (B_2)	0.597	39
1103	1104	Ar substituent str, 7a (A_1)	0.255	60

[a] Mode assignments for all the listed aromatic ring modes on the basis of an approximate C_{2v} symmetry for the *p*-nitrobenzoate group using the extensive correlations compiled by Varsanyi. (Varsanyi, G. "Assignments for Vibrational Spectra of Benzene Derivatives"; Wiley: New York, 1974.) The symmetry species of each vibration is given in parentheses.

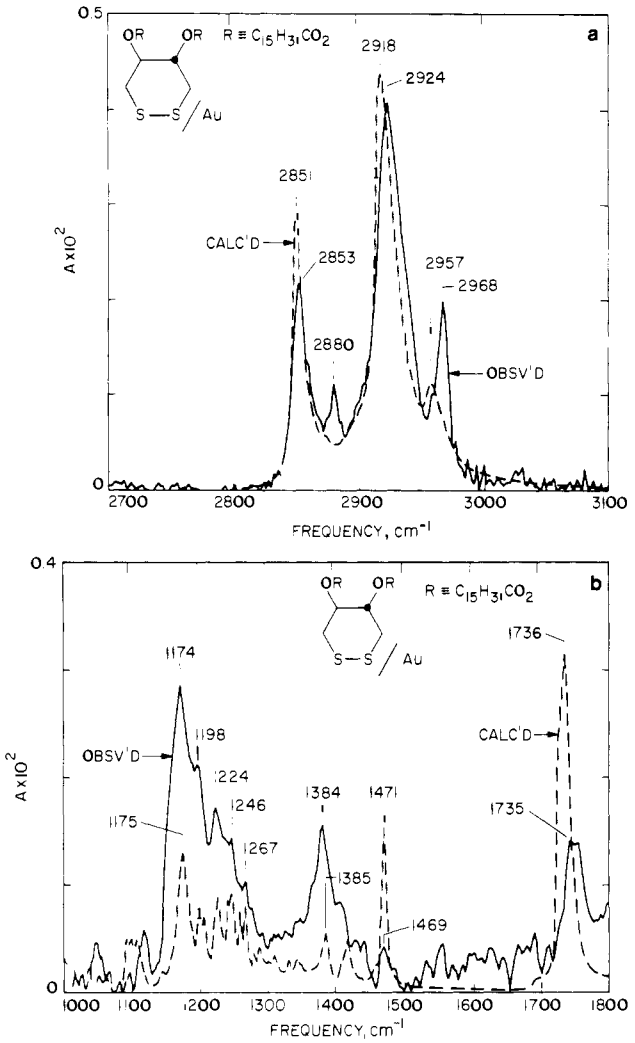

Figure 4. (a) Infrared spectra for DTT-hexadecanoate in the high-frequency region (see text): (- - -) calculated reflection spectrum; (—) observed spectrum. (b) Infrared spectra for DTT-hexadecanoate in the lower frequency region (see text): (- - -) calculated reflection spectrum; (—) observed spectrum.

same spectra will be discussed in detail in a later section as regards interpretation of adsorbate molecular structure. Specific peak positions and mode assignments are given in Tables II–IV. For HDDS and DTT-PNB, spectra are reported only for the CH stretching region of the former and the lower frequency region of the latter. For the case of HDDS the region between ~800 to 2700 cm^{-1} showed no visible peaks above the noise. In particular, attempts were made to observe absorption from a well-defined CH_2 scissors deformation, but in no case was the noise level sufficiently low to allow a definitive assignment to be made. Similarly, the aromatic and aliphatic CH stretching vibration intensities of the DTT-PNB derivative were too weak to allow a quantitative interpretation of the bands. The mode assignments for all the molecules studied were generally made by analogy with assignments for similar structures, and other relevant details are given in the tables.

An informative way to interpret these spectra is by comparison with reference spectra of a pure phase of the adsorbate material. In this way differences between reference and adsorbate spectra can be interpreted, in suitable cases, in terms of structural differences between the reference and adsorbed film states. Since all the molecules whose vibrational spectra are reported in this study are crystalline solids at room temperature, this state was chosen as a reference state. Spectra were measured by transmission through pellets prepared by pressing dispersions of the compounds in KBr matrices. In order to make these spectral comparisons quantitative, it is necessary to correct for differences

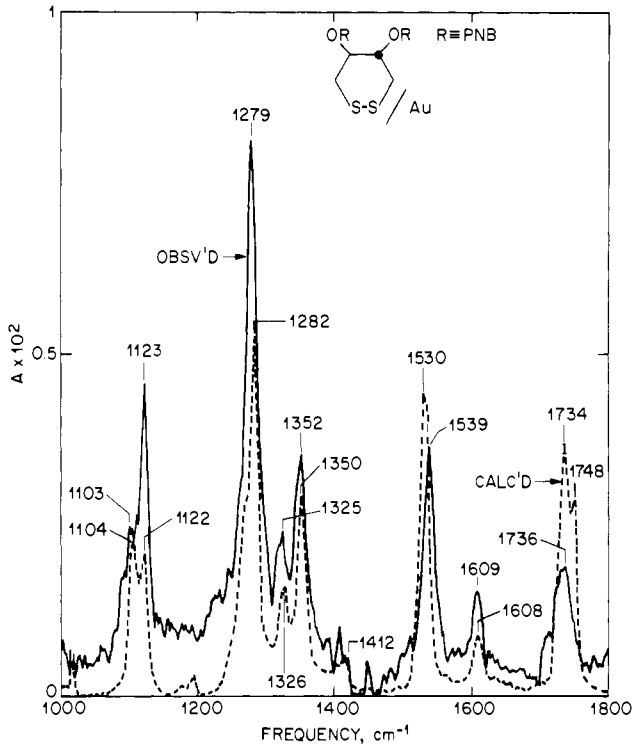

Figure 5. Infrared spectra of DTT-PNB in the lower frequency region (see text): (- - -) calculated reflection spectrum; (—) observed spectrum.

in optical dispersion distortion effects between the reflection and transmission spectra.

The approach adopted in this study involves the quantitative calculation of a reflection spectrum of a given molecule for a hypothetical model structure involving a selected thickness of a uniform film of randomly oriented bulk crystallites on a gold substrate. The model spectra are calculated from classical electromagnetic theory for a parallel layer model using the experimental geometry of the reflection spectroscopy measurements and experimentally determined values of the optical constants for gold and the bulk crystalline phase of the organic. Details of the calculation procedure and the model are given elsewhere.[9] The optical constant is defined by the equation $\hat{n} = n + ik$, where $\hat{n}$ is the complex optical constant, n is the real refractive index, and k is the absorption index.

Data for gold are taken from the literature;[13] the average values of n and k used are 3.8, 50 and 1.0, 29 for the spectral regions 1000–1800 and 2500–3100 cm^{-1}, respectively. Values of $\hat{n}$ for the organic materials were calculated from the KBr matrix transmission spectra using a previously reported[9] iterative numerical procedure in which values of k are estimated from the transmission spectra and values of n are calculated from a Kramers–Kronig transform. The values of the real refractive index at nonabsorbing frequencies (n_∞) were estimated to be ~1.45 for all the compounds studied, a value used previously for long-chain alkanoic acids.[9] The calculated spectra are shown in Figures 3–5 and values of the calculated peak frequencies are given in Tables II–IV.

Careful comparison of peak frequencies and line shapes between observed and calculated spectra show a close correspondence and imply that adsorption has little effect on the integrity of the chemical bonds in the molecules. However, the small differences in line shapes and peak frequencies which exist can be significant in terms of structural features of the monolayer assembly, such as orientational ordering and intermolecular interactions, which are different from those features of the bulk crystalline phase.

(13) Ordal, M. A.; Long, L. L.; Bell, R. J.; Bell, S. E.; Bell, R. R.; Alexander, R. W.; Ward, C. A. *Appl. Opt.* **1983**, *22*, 1099–1119. Bennett, H. E.; Bennett, J. M. In *Optical Properties and Electronic Structure of Metals and Alloys*; Abeles, F., Ed.; North-Holland: Amsterdam, 1966; p 175.

Comparison of the observed and calculated peak frequencies for the d^+ and d^- modes for HDDS and DTT-hexadecanoate shows shifts of 0 and -2 cm^{-1} and $+1$ and $+6$ cm^{-1}, respectively. This can be interpreted qualitatively as meaning that the monolayer of HDDS is packed in a solid crystalline-like environment, similar to that of the material in the KBr dispersion. However, the higher d^+ mode position in the DTT-hexadecanoate spectrum suggests an adsorbed state with significantly more disorder than that found in the crystalline state of the compound in the KBr dispersion. The lower frequency absorptions are quite informative for DTT-hexadecanoate. The collection of sharp features between ~1200 and 1300 cm^{-1} are attributed to the wag–twist progressions of the CH_2 groups of alkyl chain.[14] These arise when the alkyl chain has an all-trans zig-zag conformation and are evidence for this structure in the monolayer.[14] The changes in the C=O stretching absorption line shape (Figure 2) indicate, qualitatively, a change in the environment of the ester group in the monolayer relative to the bulk solid phase. A more detailed discussion of the structural implications of these spectra will be given in the Discussion.

Intensity differences between calculated and observed spectra can also be interpreted in terms of the monolayer structure. One contributing effect on these intensity differences is the orientation of the transition dipole moment associated with each different mode with respect to the electric field of the probing light. At a metal surface, the only significant component of the oscillating electric field is perpendicular to the surface. This gives rise to the so-called surface selection rule.[15] It follows then that $I \propto \cos^2 \phi_{mz}$, where I is the absorption intensity and ϕ_{mz} is the angle between the transition dipole (**m**) and the surface normal (**z**). Since the calculated spectrum represents a randomly oriented, isotropic film, ϕ_{mz} can be calculated from the expression

$$\cos \phi_{mz} = (I_{obsd}/3I_{calcd})^{1/2} \quad (1)$$

where I_{obsd} and I_{calcd} are the observed and calculated band intensities for a particular mode. This quantity is tabulated in Tables II–IV and was calculated on the basis of peak heights except where changes in line width between observed and calculated bands dictated a comparison of integrated intensities, as noted in the tables. Also given in the tables are values of the angle ϕ_{mz}. Before the intensity differences for any particular mode can be interpreted correctly in terms of orientational effects in the monolayer, it must be first concluded that there are no differences between the absolute magnitudes of the transition dipole moments (dynamic charge distributions) of the mode for the bulk and adsorbed states of the molecules. Such a conclusion seems reasonable for modes for which calculated and observed peak positions and line shapes are the same. In general, this should be true for those modes associated with functional groups not attached directly to the substrate surface. Since the bulk of the evidence in this study is consistent with the adsorption of these molecules via attachment of the S atoms at the gold surface, we concluded that the tabulated values of ϕ_{mz} are reasonably valid. Significant exceptions that will be discussed in detail later are the C=O stretching modes in DTT-hexadecanoate and DTT-PNB (see above), and the NO_2 asymmetric stretching mode in DTT-PNB. We will also show that detailed interpretations of the orientations associated with the CH stretching modes of the CH_3 groups in HDDS and DTT-hexadecanoate are also not straightforward, implying a perturbation of their environment in the adsorbed state relative to the bulk.

In order to relate the values of ϕ_{mz} to molecular geometry at the interface, it is necessary to define the transition dipole moment in terms of molecular coordinates. This is done in Table V for those selected modes for which reasonable assignments could be made.

Chemical Reactivity of Formed Films. Several chemical treatments were performed to examine the reactivity and stability of the films both with regard to simple dissolution of the monolayer by disruption of the substrate–adsorbate bonds and to chemical reaction of specific groups in the adsorbed molecule.

Attempts were made to remove the films by solvent rinses and chemical displacement. In general, solvent rinses had no measurable effect on ellipsometry thicknesses. Experiments in which hexadecyl disulfide films were immersed in chlorobenzene for ≳24 h, however, sometimes resulted in a partial removal of the film. Heating experiments were performed both in N_2 atmospheres and in vacuo and are presented in another section.

Attempts were made to displace films by I^- and CN^- ions, reagents with known strong affinities for gold.[16] Aqueous KI

Table V. Estimated Directions of Selected Transition Dipole Moments[a]

mode[b] (in order of decreasing frequency)	groups[c]	direction of M relative to molecular coordinates
r_a^-	alkyl chain	⊥ C–CH_3 bond, ip cc backbone
r_b^-	alkyl chain	⊥ cc backbone plane
r^+ (FR)	alkyl chain	∥ C–CH_3 bond
d^-	alkyl chain	⊥ cc backbone plane
d^+ (FR)	alkyl chain	⊥ chain axis, ip cc backbone
r^+	alkyl chain	∥ C–CH_3 bond
d^+	alkyl chain	⊥ chain axis, ip cc backbone
C=O str	DTT ester	∥ C=O bond
8a	$ArNO_2$	⊥ axis through C–NO_2, C–CO_2 bonds (ring positions 1, 4)
NO_2 asym str	$ArNO_2$	∥ axis through O atoms
CH_2 scissors def	alkyl chain	⊥ chain axis, ip cc backbone
NO_2 sym str	$ArNO_2$	∥ axis bisecting ONO angle
14	$ArNO_2$	same as 8a
C–O str	DTT ester	*d*
18b	$ArNO_2$	same as 8a
7a	$ArNO_2$	∥ axis through C–NO_2, C–CO_2 bonds (ring positions 1, 4)

[a] Directions are approximated from the normal mode descriptions. Exact directions could be as much as several degrees off those calculated from the normal mode potential energy distributions and need to be determined from charge distribution calculations. [b] More detail is found in Tables II–IV. [c] Groups located in the three compounds HDDS, DTT-hexadecanoate, and DTT-PNB; $ArNO_2$ is the nitrophenyl group. [d] The transition moment direct is probably *not* along the C–O bond because of the complex coupling of other modes with the C–O stretch: Boerio, F. J.; Bahl, S. K. *Spectrochim. Acta, Part A* **1976**, *32*, 987–1006.

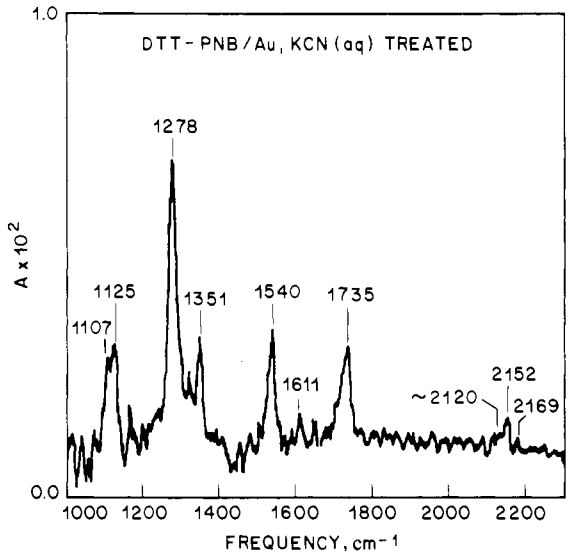

Figure 6. Infrared spectrum showing the coadsorption (and partial displacement of) of DTT-PNB and cyanide ion on a gold surface. The sample was prepared by immersing a DTT-PNB sample into an aqueous cyanide solution for 24 h followed by rinsing. Mode assignments are described in the text.

(14) Snyder, R. G. *J. Mol. Spectrosc.* **1960**, *4*, 411–434.
(15) Greenler, R. G. *J. Chem. Phys.* **1966**, *44*, 310–335.
(16) *Handbook of Thin Film Technology*; Maissel, L. I., Glang, R., Eds.; McGraw-Hill: New York, 1970, pp 7–37.

solutions tended to remove and/or corrode the gold substrate films. An experiment with a DTT-PNB/Au sample in which the film was soaked for 24 h in an ~1 M KCN solution at room temperature resulted primarily in the adsorption of CN^- on the gold surface concurrent with a partial displacement of the disulfide. Conclusive evidence for this was obtained by infrared spectroscopy. Figure 6 shows the reflection spectrum of a CN^--treated sample after its removal from aqueous KCN solution followed by several water rinses, and drying by spinning. A comparison of the untreated and CN^--treated films, shown in Figure 5 and 6, respectively, reveals a small drop in overall spectral intensity and slight changes in relative peak heights after the CN^- treatment. From the intensity change it is likely that partial film removal has occurred (~20%). While there are no significant changes in peak frequencies associated with the DTT-PNB spectrum, a new absorption appears at 2152 cm^{-1} with a possible additional band at 2169 cm^{-1} and an apparent shoulder at ~2120 cm^{-1} also being observed. These absorptions can be associated with adsorbed CN^- species. The coverage of the CN^- species was estimated from a calculation of absorption intensity for a hypothetical thin film of $K[Au(CN)_2]$. This salt shows a maximum absorption at 2146 cm^{-1} which is attributed to the CN^- stretching mode. The optical constants in this region were determined from a pressed KBr pellet. The calculated integrated reflection spectral intensity matches the experimental determined value shown in Figure 6 for a hypothetical 1–2-Å film of the $K[Au(CN)_2]$. Thus one can conclude that CN^- can slowly displace DTT-PNB and perhaps even intercolate into available sites (defect) within the DTT-PNB covered areas on the gold.

Experiments to determine the effects of film structure on the chemical reactivity of adsorbate molecular groups were performed for DTT-hexadecanoate films. The susceptibility of the ester group toward transesterification was checked using treatments with methanol/acetic acid (HOAC) and ~0.1 M $NaOCH_3$ in CH_3OH solutions. The extents of reaction were followed by infrared spectroscopy. The CH_3OH/HOAc solution had no measurable effect on the spectrum, even after several days immersion at ~20 °C. The stronger conditions of a $NaOCH_3/CH_3OH$ solution immersion for 24 h also had no measurable effect. The latter conditions are sufficient to completely cleave the ester group in solution, and one can conclude that the ester group in the film is probably protected from attack by the methoxide nucleophile by the strongly hydrophobic alkyl chains.

XPS Studies of the Nature of Disulfide Bonding to Gold Surfaces. The adsorption of a closest packed monolayer of HDDS on a gold surface does not result in a significant perturbation of the Au 4f core level spectrum determined by XPS. Though the total integrated spectral intensity decreases, a result expected owing to the presence of a relatively thick (~20 Å, see above), attenuating organic overlayer, such features as the full width at half-maximum and the Au $4f_{7/2}$ (referenced at 84.0 eV) and $4f_{5/2}$ binding energies remained unchanged. Careful examination of these same spectra also did not reveal new "asymmetries" in the line shape which might be ascribed to gold–sulfur bonding. Examination of the spectrum in the S 2p region showed an extremely broad and highly asymmetric (under the acquisition conditions employed, this core level is an unresolved, spin–orbit-coupled doublet and is believed to contain spectral contributions from more than one form of chemisorbed disulfide) peak with a binding energy maximum at ~162.7 eV (see Figure 7). It is of interest to note that this value is typical of most disulfides on gold.[17] Further comment will be deferred to the Discussion.

XPS and Reflection Infrared Spectroscopy Studies of the Thermal Chemistry of Organic Disulfide Monolayers on Gold. When a disulfide monolayer is heated above a certain temperature range (see below), significant changes are effected in the adsorbed film as determined by both XPS and IR. The most striking changes are evidenced by XPS at temperatures in the range of 170–230 °C. The character of these observations is shown

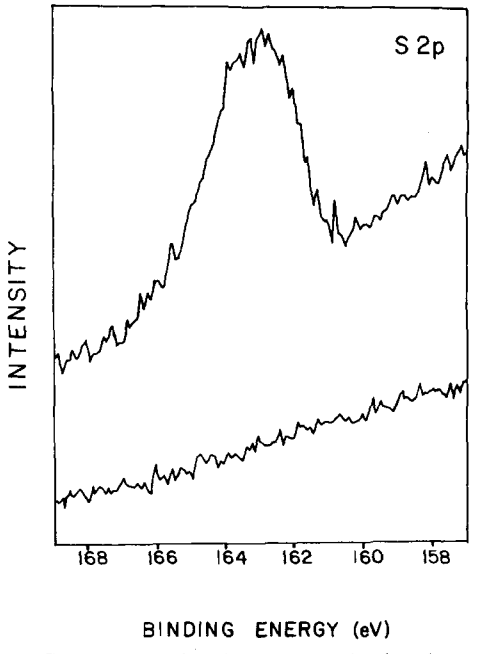

Figure 7. XPS spectra showing the S 2p core level region of a di-*n*-hexadecyl disulfide monolayer on gold before (upper trace) and after (lower trace) heating the sample to ~225 °C. The spectral intensity in the lower trace is normalized to that in the initial monolayer before heating. To improve sensitivity a lower instrumental resolution of ~1.5 eV was used.

graphically in Figure 7, which shows, for a film of hexadecyl disulfide, the clear loss of sulfur from the gold surface when the sample is heated to 225 °C. Examination of the C 1s core level region of the spectrum shows that the hydrocarbon portion of the molecule is lost as well, and presumably desorbs, from the surface at temperatures of this order. Our qualitative observations suggest that, of the classes of structures reported in Table I, the most stable monolayers are formed from linear aliphatic adsorbates such as HDDS. The acylated derivatives of DTT-H consistently were much less stable toward heating, decomposing at the lower end of the range cited above. Careful monitoring of the S 2p core levels during a slow heating cycle did not reveal the formation of new, sulfur-based adsorbate structures. Rather, the integrated S 2p intensity decreased without intermediate changes in binding energy and line shape being observed. This result suggests that, at least for HDDS, the surface bonding involved in the formation of the overlayer at ambient temperature persists to temperatures where the adsorbate desorbs.

A qualitative estimate of adsorbate bond energy can be made from observations of the time required for desorption at a given temperature. Assuming first-order kinetics and an A factor of $\sim 10^{13}$ s^{-1} (no change in degrees of freedom in the desorption transition state), the observed approximate 50% desorption, which occurs in the range of minutes at 200 °C, gives rise to calculated activation energies in the range of 30–35 kcal/mol. This value is in close agreement with the results of other studies to be reported separately which examine the thermal desorption of dimethyldisulfide adsorbed on a Au(111) single-crystal surface.[17] We thus conclude that, at least for linear, aliphatic adsorbates, the dominant process involved in this thermal chemistry is the disruption of the gold–sulfur bond to give a disulfide desorption product, and not adsorbate decomposition. An interesting exception in this regard was found with a DTT-PNB/Au sample. This sample was covered by a well-cleaned watch glass and heated to ~150 °C in an $\sim 10^{-8}$-torr vacuum. Under these conditions a faint, purple color appeared on the cooler watch glass. The color was removed by solvent rinses, e.g., acetone. Since no color forms without an adsorbed film on the gold, we conclude that at ~150 °C the DTT-PNB monolayer decomposes to a volatile, intensely colored material.

Infrared spectroscopy studies of HDDS films under a N_2 atmosphere showed stability toward desorption until temperatures

(17) Nuzzo, R. G.; Zegarski, B.; Dubois, L. H. *J. Am. Chem. Soc.* **1987**, *109*, 733–740.

at or near 200 °C where all spectral characteristics were lost irreversibly. This finding is also consistent with a simple desorption process as described above. Below 150 °C, however, heating causes spectral changes even though our analysis indicates that no significant loss of material from the film occurs. The only spectral features of appreciable intensity are those of the d^+ and d^- CH_2 modes in the C–H stretching region so only these were monitored in the heating experiments. From room temperature up to 100–125 °C, no change in the maximum absorption frequencies occurred within the limits of experimental error. The line widths at half-maximum height increased slowly between ambient and 99 °C, from 9 to ~11 cm^{-1} for d^+ and from 11 to ~18 cm^{-1} for d^-. Upon heating further to 125 °C, the line widths jumped from 11 to 18 cm^{-1} for d^+ and 18 to 31 cm^{-1} for d^-. Upon cooling to ambient, the respective line widths decreased to 12 and 13 cm^{-1}, values just slightly larger than those observed originally. Upon reheating to 125 °C, the line widths increased to 20 and 32 cm^{-1} and a slight peak shift of +3 and +2 cm^{-1} occurred for the d^+ and d^- modes, respectively. Upon further heating to 150 °C the peaks shifted an additional +1 cm^{-1} and the line widths *decreased* to ~16 at 22 cm^{-1}, respectively. Upon cooling to ambient, the peak positions did not change and the line widths decreased slightly to 15 and 19 cm^{-1}. Taken together, these results indicate that some form of thermally induced structural change (presumably a disordering) occurs reversibly near ~125 °C; at ~150 °C the changes which occur are irreversible and may reflect a partial desorption of the adsorbate or restructuring of the substrate. Differential scanning calorimetry (DSC) measurements showed a sharp melting point of 53.9 °C for the pure compound. Clearly, then, the surface-bound molecules exhibit a thermal behavior completely different from the bulk material.

In comparison, heating a monolayer sample of DTT-hexadecanoate on Au between ambient and 150 °C produces only small shifts in the peak frequencies and line widths. For the d^+ and d^- modes, respectively, the peak frequencies gradually change by +3 and +5 cm^{-1} and the line widths by +2 and −1 cm^{-1}. Upon cooling to ambient, the peak frequencies shift by −1 and −5 cm^{-1} while the line widths change +1 and −3 cm^{-1}. These changes are reasonably small relative to experimental error (<±1 cm^{-1} in peak frequencies and line widths) and suggest that no major changes in structure occur with thermal treatment below 150 °C. The melting point of the pure material by DSC measurements is 64.4 °C. This behavior suggests that the alkyl chains cannot disorder significantly beyond that which characterizes the ambient state until desorption occurs at temperatures above 150 °C. Such a result is consistent with a liquid-crystalline-like nature (loose, oriented lattice) for the DTT-hexadecanoate chains at ambient temperature (see below for a more detailed discussion).

Radioisotropic Labeling Studies. Evidence for high site densities in organic disulfide monolayers on gold surfaces was obtained using tritiated derivatives of oxidized DTT-H. A preformed, tritium-labeled bisacetate derivative of DTT-H (methyl-^{3}H) showed that formal site densities of 4.4×10^{14} molecules cm^{-2} are obtained for this adsorbate. This result is approximately twice that predicted from calculations based on space-filling models. We believe that two sources of error are likely to be involved. First, these surfaces are not atomically smooth; estimates based on high-resolution SEM and TEM analyses suggest ~1.3 as a reasonable roughness factor for the substrates used (see section below on surface morphology). Second, we do not know the exact scintillation counting efficiencies for tritium-labeled adsorbates on a metal surface. Our calculations employed the reasonable estimate of solution-counting efficiencies corrected for the 1Π geometry of labels at a surface (electrons emitted into the sample not being observable). Thus, the results obtained can only be approximate, as the true correction factors are expected to be sensitive to surface roughness. Despite this limitation, the data, which push toward overly large coverage values, strongly argue for a dense or close-packed arrangement in the adsorbed layer.

We note, with some interest, that attempts to directly acetylate DTT-H while coordinated to the gold surface consistently gave lower measured site densities. This, we feel, reflects strong steric preclusions to high acetylation yields at this "two-dimensional" interface.

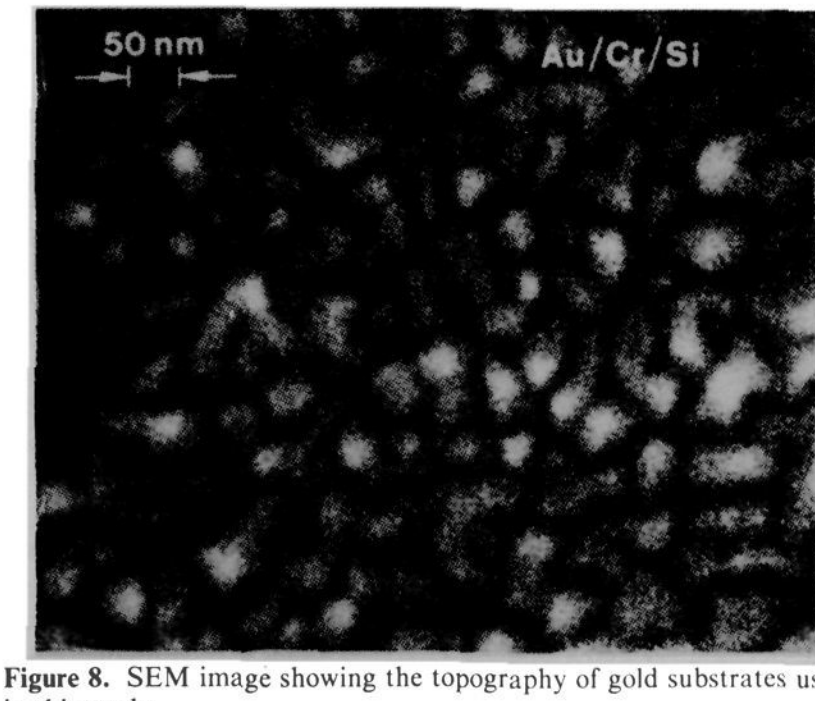

Figure 8. SEM image showing the topography of gold substrates used in this study.

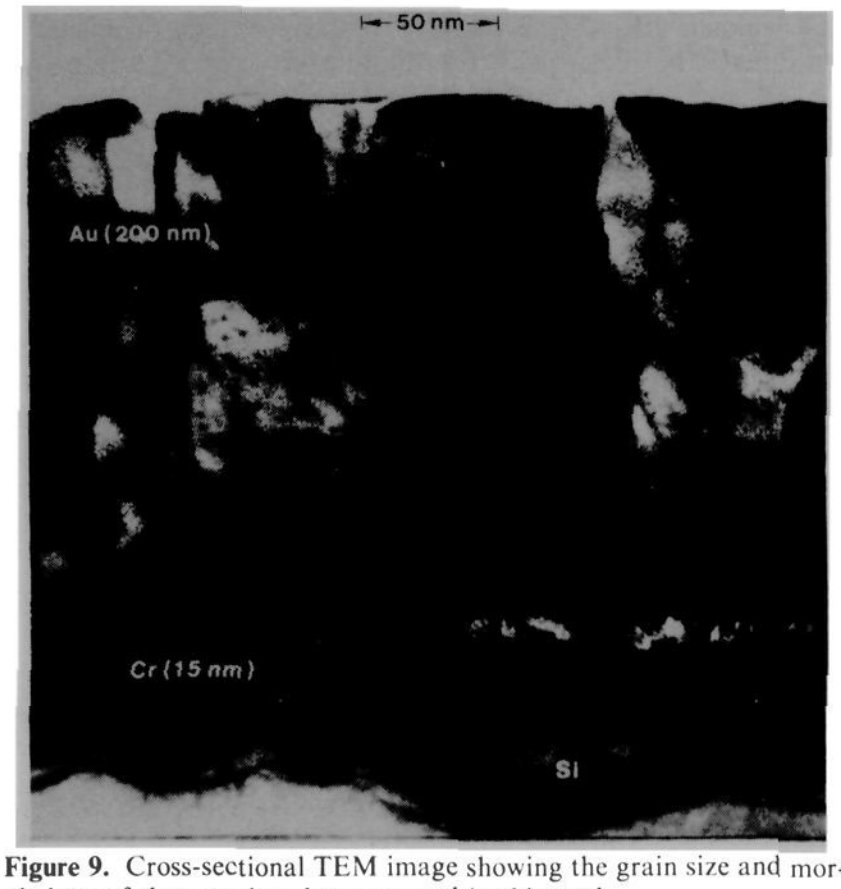

Figure 9. Cross-sectional TEM image showing the grain size and morphology of the sample substrates used in this study.

Substrate Morphology. The morphology of the evaporated gold films was characterized by SEM, TEM, and X-ray diffraction. Figure 8 shows an SEM image of a typical sample substrate. From this image, one can estimate that the surface features consist of shallow (~50 Å) hill-like variations of sample thickness whose periodicity ranges around several hundred angstroms. In Figure 9 is shown a high-resolution TEM image of a cross section of a sample. This image confirms and expands the general notions developed from the SEM data described above. The surface is not atomically smooth but, rather, shows subtle variations of thickness (i.e., "rolling hills") which result from the complex, polycrystalline nature of the film. The average grain size is of the order of ~500 Å and, most significantly, the intergrain surface area appears to be extremely smooth (suggesting the presence of long-ranging terraces).

X-ray diffraction provides additional information about the crystallographic texture of these polycrystalline Au substrates. Our results suggest that these films have an *extremely strong* (111) texture. We have not been able to quantify this rigorously, but, based on models and analyses of bulk gold samples, estimate that at least 80% of the sample is exhibiting a preferred (111) orientation. This large degree of (111) faceting is also supported by the results of underpotential electrochemical deposition experi-

ments with Pb–Pb(II) on these polycrystalline films.[18]

Discussion

The bulk of the experimental evidence in this study supports a general description of multifunctional organic disulfide films on gold surfaces with the following features: (1) a relatively strong adsorbate–substrate interaction involving attachment via sulfur atoms; (2) high surface coverages near bulk condensed-phase densities; (3) orientational ordering with the center of mass of the adsorbate molecules located away from the surface and terminal functional groups extending toward the ambient interface. In addition to these general features, each type of adsorbate film exhibits specific conformational and intra- and intermolecular structural features different from that found in the bulk materials as well as specific molecular orientations with respect to the surface.

Perhaps one of the most interesting aspects of this study is the repeated strong preference for the disulfide group to attach to the gold surface relative to a wide variety of polar and nonpolar groups including hydroxyl, amino, carbonyl, chloro, alkyl, phenyl, and nitro (other evidence suggests that even other sulfur-containing functional groups such as thiols and sulfides also are considerably less competitive in the adsorption process relative to disulfides).[8,17,19] This conclusion implies that molecules can be chosen specifically to present a given functional group of interest to the ambient interface to impart desired physical and chemical properties to the sample surface. Evidence for variation of physical properties can be seen by the variation of contact angles with structure as has been described in an earlier communication.[8] In addition, other studies involving polymer adsorption give direct evidence for hydrogen-bonding interactions between carbonyl-containing polymers and adsorbed hydroxy disulfides such as dithiothreitol.[20] An example of surface chemical reactivity is given by the smooth reaction of tritiated acetic anhydride with a DTT-H monolayer in good, but not quantitative, yields as described above. An example from another study to be reported demonstrates efficient reactions of isocyanates with amino groups in adsorbed aminoalkyl dislufides.[21] These vignettes suggest the most intriguing feature of this unique chemisorption system, namely, the ability it provides to construct model organic solids with well-defined surfaces. In reports soon to be described by these and other workers, this feature will be widely exploited to develop the surface and interfacial chemistries of organic materials. For the present, however, we will restrict our discussion to the organizational characteristics and bonding which results when structurally complex organic disulfides adsorb on gold.

The binding of the disulfide group to the gold surface is surprisingly strong in view of the general inertness of gold toward the chemisorption of organic compounds.[8] Thermally induced desorption of HDDS and DTT-hexadecanoate does not occur at appreciable rates until temperatures of the order of 180–200 °C are reached as shown by both the IR and XPS experiments described above. Thermal desorption involves complete removal of the surface film as evidenced by the loss of the S 2p core level binding energy peak in the XPS spectra (Figure 7) and the organic moiety absorptions (the alkyl group) in the IR spectra. From our desorption data, an estimate of 30–35-kcal/mol for the adsorption bond energy can be made. Detailed thermal desorption studies of short-chain alkyl disulfides to be reported shortly suggest, in close agreement with these estimates, adsorption energies of ~28 kcal/mol.[17] Degradation of the molecular structure may occur at lower temperatures for appropriate molecules such as DTT-PNB, which forms a film susceptible to decomposition at ~135 °C with the concomitant formation of a colored degradation product. Some measure of the strength of the surface bond toward displacement is shown by the observed inertness of a DTT-PNB film toward aqueous cyanide ion. Aqueous cyanide readily adsorbs on the gold surface (see Figure 4), but the infrared evidence suggests that no more than a small fraction (<20%) of the disulfide is displaced.

The exact chemical stability of the adsorbed S–S group is unclear from the results of this study. In a separate paper, the nature of the bonding of dimethyl disulfide on an Au(111) single-crystal surface in UHV has been definitively characterized.[17] A complex adsorbed state was found at high coverage which was comprised principally of dissociatively chemisorbed disulfide, although the presence of some residual molecular (i.e., nondissociated) disulfide was clearly indicated.[17] The close correspondence of the XPS and desorption data, reported above, to the results on Au(111) strongly indicates that the dominant adsorption process, at least for HDDS, is dissociative in character. In addition, surface-enhanced Raman spectroscopic results of disulfide adsorption on gold films[22] and gold islands[23] show a loss of the S–S stretching vibration on adsorption and are consistent with dissociative adsorption.

Under the conditions of solution deposition, the coverages obtained for the variety of disulfides studied are consistently close to that of a closest packed monolayer. This conclusion is supported by ellipsometry, contact angle, radioisotope labeling, and infrared analysis. Consideration of the results from all these techniques together suggests that coverages are better than ~90% of a closest packed monolayer. The kinetics of adsorption were not followed directly, but qualitative observations show that near-complete coverages can be obtained in many cases within a few minutes. Such observations indicate a high degree of surface mobility for adsorbate species in the range of low to intermediate coverages. Their identity, viz., dissociated or nondissociated disulfide, cannot be determined from the data currently available to us. It seems likely, however, that all chemisorbed groups must possess reasonable mobility in order for the assembled phases to ultimately reach a bulk-like density (see below). Electrochemical experiments, which are sensitive to film defects, show that full packing is not obtained usually until after several hours of incubation.[19b] Specific experiments with long-chain (C_{16} and longer) thiols[19b] show that coverages exceed 99% and that charge-transfer processes to the gold electrode are diminished in efficiency by several orders of magnitude. Evidence for high packing densities is also given indirectly in the present study by infrared spectral line shapes and peak positions for the cases in which the spectral interpretations involve intermolecular interactions for specific molecular groups, in particular, alkyl chains and the aromatic nitro groups in HDDS, DTT-hexadecanoate, and DTT-PNB, respectively (see below for a detailed discussion).

In general, the adsorption process seems to have no effect on the integrity of the chemical bonds in the disulfide molecules with the possible exception of the disulfide linkage which may be cleaved (see above discussion). The generally close correspondence of the vibrational modes in the film and bulk infrared spectra support this conclusion quite firmly. An interesting contrast is the adsorption of disulfides on polycrystalline silver and copper(100) where surface-enhanced Raman[24] and high-resolution electron energy loss spectroscopies,[25] respectively, indicate that some degree of C–S bond cleavage occurs in the adsorbed states. In the case of adsorption on copper, C–S bond cleavage is quite pronounced.

The intermolecular and intramolecular interactions in the surface assemblies are qualitatively similar to the bulk solid state, but some specific differences do exist as shown by careful interpretation and comparison of infrared spectra for these two phases.

The two C16 alkyl-substituted disulfides, HDDS and DTT-hexadecanoate, show spectral features which can be interpreted in terms of their alkyl-chain environments and conformations. For HDDS the CH_2 symmetric (d^+) stretching mode is unshifted

(18) Porter, M. D.; Allara, D. L., unpublished results.
(19) (a) Troughton, B.; Whitesides, G. M., personal communication. (b) Porter, M. D.; Allara, D. L.; Chidsey, C. E. D. *J. Am. Chem. Soc.*, accepted for publication.
(20) Allara, D. L., unpublished results.
(21) Ratner, B. D.; Brown, W.; Allara, D. L., unpublished results.
(22) Allara, D. L.; Murray, C. A., unpublished results.
(23) Sandroff, C. J., personal communication.
(24) Sandroff, C. J.; Hershbach, D. R. *J. Phys. Chem.* **1982**, *86*, 2700–2704.
(25) Sexton, B. A.; Nyberg, G. L. *Surf. Sci.* **1986**, *165*, 251–267.

relative to the corrected bulk crystalline phase peak, while the antisymmetric mode (d^-) is shifted by -2 cm^{-1} (see Table II). These shifts indicate that the monolayer packing environment of the alkyl CH_2 groups is similar to that of the bulk crystallites in the KBr dispersion. In fact, the downward shift of the d^- mode and its narrower line width in the monolayer (see Figure 1) suggests an even tighter packing relative to the bulk. These conclusions are based on a number of studies in which these peak frequencies and line widths correlate quite consistently with the ordering of the alkyl chains for a variety of alkanes and alkyl-substituted molecules.[26] For example, the d^+ and d^- modes of a polymethylene chain in the crystalline state appear at 2850 and 2920 cm^{-1}, respectively, while in the liquid state they shift to 2856 and 2928 cm^{-1}.[26]

On the other hand, the case of DTT-hexadecanoate is interesting because the CH_2 modes exhibit increased d^+ and d^- frequencies (+2 and +6 cm^{-1}, respectively; see Table III) and line widths (+6, and +7 cm^{-1}, respectively) relative to the corrected, bulk crystalline-phase values. From the above discussion, such shifts would indicate that, on average, the chains in the DTT-hexadecanoate monolayer are in an environment allowing increased chain mobility compared to the solid, crystalline environment of the bulk. The upward frequency shifts of the d modes which occur during the melting of bulk, crystalline polymethylene chains can be attributed to the appearance of gauche conformations.[26] In the present case, however, the presence of the progression of wagging and twisting modes in the lower frequency spectrum (Figure 4b) indicates that the chains are primarily in an all-trans conformation and, thus, are not conformationally disordered to a significant extent. The frequency shifts observed for DTT-hexadecanoate thus would appear to be associated with an environment of reduced chain–chain interactions associated with larger amplitude thermal motions[27] as compared to the crystalline bulk-phase structure. The local environment around the ester group is also somewhat different in the monolayer than in the bulk as judged by the significant difference in line shapes (see Figure 2) for the C=O stretching mode absorption. The lower frequency contribution to the C=O band (a poorly resolved shoulder which is absent in solution) of the corrected solid-phase spectrum is greatly reduced in the monolayer while a higher frequency component appears in the monolayer band. The physical nature of this change cannot be determined from these data alone, but does suggest significant differences in the relevant molecular interactions.

In the case of the DTT-PNB monolayer, the correspondence of the corrected bulk solid phase and monolayer spectral frequencies is quite close (see Table IV), usually within ±2 cm^{-1}, except for the asymmetric NO_2 group stretching mode absorption. For the latter, the monolayer frequency is 9 cm^{-1} higher than the corrected bulk phase frequency. This suggests some differences in the local environment of the NO_2 group in the two phases. Further evidence for such a perturbation is given by the discrepancy in the orientational information given by the ring modes and the NO_2 modes (see discussion below).

An important factor in determining the formation and properties of the monolayers is the orientation of the molecules on the substrate. All the evidence in this study indicates attachment to the surface by the S atoms. The remainder of the molecule should be free to orient in or toward the preparation solution, limited only be considerations of conformational, intermolecular, and interfacial free energies. The molecular surface orientation can be derived in principle from the infrared intensities provided that the vibrational mode frequencies and intensities are not significantly perturbed by other structural factors. The calculated surface orientations (ϕ_{mz}) of the transition dipole moments of a number of modes are given in Tables II–IV. In most cases, each of these values of ϕ_{mz} are associated with a specific molecular group. The overall surface orientation of a molecule can be determined, then, from the relationship between the molecular group coordinates and the surface coordinates.

Table VI. Orientation[a] of C–H Modes for Adsorbed HDDS

mode ($\bar{\nu}$)	angle of M from surface normal: calcd[b] from spectra	from model[c]
r_a^- (2965)	0–35	80 (78)
r_b^- (2953–58)	55–59	60 (69)
r^+ (FR) (2938)	0–55	32 (24)
d^- (2918)	60	60 (69)
d^+ (FR) (2893)	42–60	70 (69)
r^+ (2878)	0–28	32 (24)
d^+ (2850)	70	70 (69)

[a] Transition moment directions in terms of molecular coordinates are given in Table V. Mode assignments are given in Table II. [b] Calculated ranges are given for bands where the intensity is uncertain because of noise and/or lack of resolution. [c] The model can be described by the following operations: an all-trans alkyl chain perpendicualr to the surface is tilted 37° away from the surface normal with the CCC backbone plane remaining perpendicular to the surface and the C–CH_3 bond becomes more parallel to the surface normal. The chain is then rotated about the chain axis by 55°. This can be seen qualitatively in Figure 10. Values in parentheses represent calculations for a model with a 30° tilt and a 45° rotation with reference to the operation in footnote *c*.

One of the obvious requirements of this approach is that different modes for the same molecular group must provide identical values of the surface orientation of the group. Exceptions to this indicate that other factors besides surface orientation are affecting the spectral intensities. Orientations were examined for three molecules: HDDS, DTT-hexadecanoate, and DTT-PNB. Relationships between the molecular and surface coordinates for selected groups in these molecules are given in Table V. From these relationships, and the values of ϕ_{mz} in Tables II–IV, surface orientations were calculated for selected modes of alkyl chains in HDDS and DTT-hexadecanoate, the ester of DTT-hexadecanoate, and several nitrobenzoate derived modes of DTT-PNB. The modes selected were chosen on the basis that reasonable estimates for the transition moment directions could be made and that the absorption frequencies and line widths associated with the modes did not appear significantly perturbed in the monolayer compared to the bulk solid phase.

The selection of a geometry for the alkyl chains of HDDS and DTT-hexadecanoate is complicated because of the existence of two chains per molecule, particularly for the DTT derivative where S–S scission still leaves the chains bonded on the same molecule. If these chains were to pack together efficiently, they could line up completely parallel to one another, with the CH_2 groups parallel but the CH_3 groups extending from the chain ends on opposite sides, or with the *c* axis of one chain rotated by 90° such that the backbone planes are mutually perpendicular (see below).

For HDDS, the best fit to the ϕ_{mz} values for the d^+ and d^- modes is an average chain tilt of 37° from the surface normal with a 55° twist around the *c* axis as shown in Figure 10. The data are given in Table VI. To illustrate the sensitivity of the calculated angles to model geometry, Table VI also shows results for a model with a 30° chain tilt and a 45° rotation. The only model which can accommodate this best fit geometry for a cleaved S–S bond is one with the chain CCC bonds parallel. Specific information on the relative orientations of the CH_3 groups in principle could be obtained from their mode intensities, but a fundamental problem exists in that inherently contradictory information is obtained from these modes. Each of the transition moments for the three CH_3 stretching modes is mutually orthogonal to the others so that the sum of $\cos^2 \phi_{mz}$ for the modes must be unity. We find, however, that this value ranges consistently between 1.5 and 2.3. This manifests itself also in the large discrepancy between the observed and calculated values of ϕ_{mz} for the r_a^- mode whereas there is no such discrepancy for the r_b^- and r^+ models (see Table II). This deviation is caused by the larger values of the observed CH_3 mode intensities relative to those calculated from the isotropic solid-phase spectra. The reason for this is not understood but could

(26) Snyder, R. G.; Strauss, H. L.; Elliger, C. A. *J. Phys. Chem.* **1982**, *86*, 5145–5150. MacPhail, R. A.; Strauss, H. L.; Snyder, R. G.; Elliger, C. A. *Ibid.* **1984**, *88*, 334–341.

(27) Snyder, R. G., personal communication.

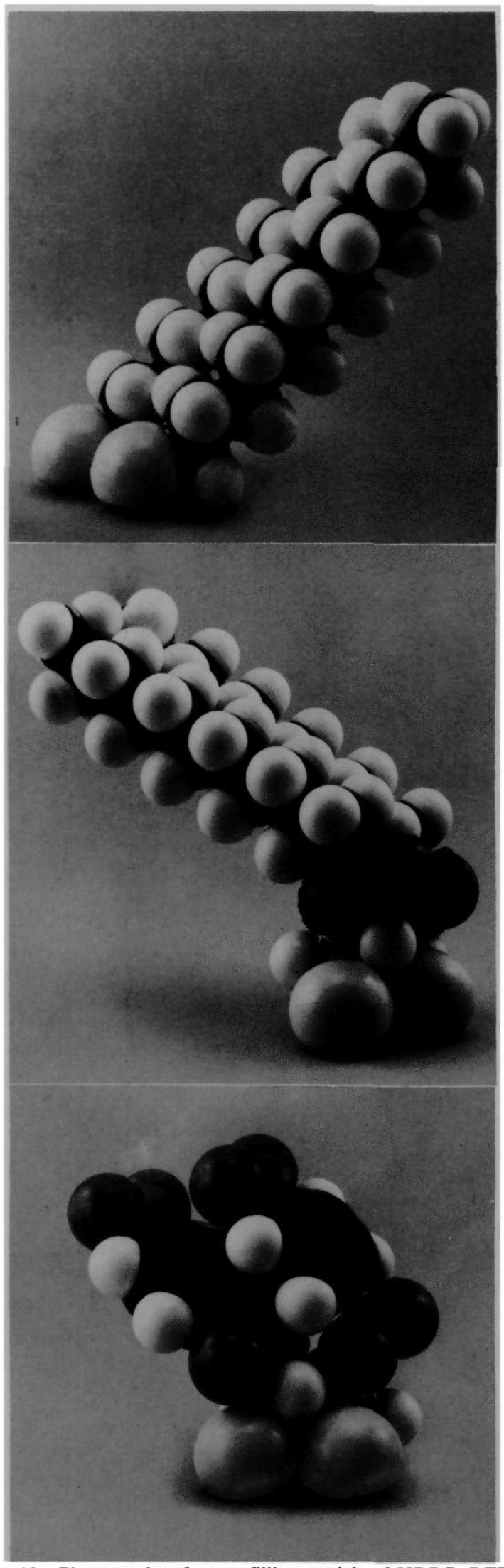

Figure 10. Photographs of space-filling models of HDDS, DTT-hexadecanoate, and DTT-PNB arranged and oriented according to the best fit describing the data in Figures 3–5, respectively. Methods of analysis used to arrive at these proposed structures are described in the text. The lengths of the polymethylene chains in the HDDS and DTT-hexadecanoate models have been shortened for reasons of clarity.

be due to some unaccounted perturbation of the transition moments or, possibly, to some inclusion of a hydrocarbon impurity in the ambient film–interface region. Neither of these possibilities seem particularly reasonable and further work is needed to sort out this fine point of the spectra.

Table VII. Orientation[a] of C–H Modes for Adsorbed DTT-Hexadecanoate

	angle of M from surface normal	
mode ($\bar{\nu}$)	calcd from spectra[b]	from model[c]
r_a^- (2968)	~0	74 (82)
r_b^- (2958)	53–63	50 (54)
d^- (2924)	49	50 (55, 59)
r^+ (2880)	0–42	44 (37)
d^+ (2853)	51	50 (55, 42)

[a] For details see footnote *a* in Table VI. [b] See footnote *b* in Table VI. [c] This model can be described by the following operations: An all-trans alkyl chain perpendicular to the surface is tilted 65° away from the surface normal with the CCC backbone plane remaining perpendicular to the surface and the C–CH_3 bond is first brought through a position parallel to the surface normal. The chain is then rotated by 45° around the chain axis. This is qualitatively shown in Figure 10. The first values in parentheses represent calculations for 55° tilt and 45° rotation and the second, where given, for 65° tilt and 35° rotation.

For DTT-hexadecanoate orientational information can be inferred from the spectra both for the alkyl chains and for the C=O bonds of the ester group. Using the CH_2 modes, the best fit of the ϕ_{mz} values in Table III is consistent with a model of parallel alkyl chains with an average tilt of 65° from the surface normal and rotated 45° around the *c* axis (see Figure 10). The details of this fit are shown in Table VII. The sensitivity of this calculation is indicated in Table VII by calculations from models with a 55° tilt and 45° rotation and a 65° tilt and 35° rotation. This best fit model requires the ester C=O bonds to be close to parallel with the surface plane. The average value of ϕ_{mz} for the C=O stretching mode (see Table III) indicates the bonds are 22° away from parallel with the surface and thus supports the tilted chain structure in Figure 10. However, alternate models with opposite C–CH_3 bond alignments or mutually orthogonal chains are also consistent with the above data and are allowed by the fairly flexible geometry of the DTT moiety. The intensities of the CH_3 modes, in principle, would distinguish among the models but, for the same reasons as was the case with the HDDS monolayer, these modes cannot be reliably used to determine further details of the chain orientation.

The information for the surface geometry of the DTT-PNB molecule comes from the NO_2, aromatic ring, and C=O vibrational modes of the *p*-nitrobenzoate group (PNB). The planar nitroaromatic ring has the ring and NO_2 mode (Table III) transition moments in orthogonal directions in the plane of the ring as shown in Table V. For the ring modes 8a, 14, and 18b, which all have transition moments parallel to the 1,4 ring axis (see Table V), the values of ϕ_{mz} are 42, 40, and 39°, all in excellent agreement with one another. However, the antisymmetric NO_2 stretching mode, which for a planar nitrobenzoate group also has a transition moment perpendicular to the 1,4 direction, exhibits a corresponding value of 52°, ~12° higher than that judged from the ring modes. This discrepancy appears especially significant as the peak frequency for the observed antisymmetric NO_2 mode is shifted by +9 cm^{-1} relative to the corrected bulk-phase value (Table IV), whereas no other mode in the monolayer spectrum exhibits a shift larger than 2 cm^{-1}. The symmetric NO_2 stretching mode and the ring mode 7a are assigned parallel transition moment directions and give values of ϕ_{mz} of 52 and 60°, respectively. It is interesting to note, however, that this particular NO_2 mode shows only a 2-cm^{-1} difference between corrected bulk and surface peak frequencies. The above evidence suggests a significant change in intermolecular interactions of the nitro group in going from the bulk phase to the monolayer film.

The most obvious difference characterizing the adsorbed state is that the NO_2 group (and even the methyls in the monolayers discussed above) is exposed at the ambient interface and experiences fewer intermolecular interactions than is the case for the bulk, condensed phase. This hypothesis is quite reasonable as can be shown by comparing the spectra of gas- and liquid-phase nitrobenzene. We measure shifts of +8 and +25 cm^{-1} for the

symmetric and antisymmetric modes, respectively, in going from the liquid to the gas phase. The model in Figure 10 shows that part of the NO_2 group is, in fact, exposed to the ambient, overlying (gas) phase.

Using the values of ϕ_{mz} for the ring modes only in order to avoid complications arising from the perturbed nitro modes, the average orientation of a nitrobenzoate group involves a 60° tilt of the ring plane away from the surface normal with an ~30° twist around the 1,4 ring axis. This is depicted in the model in Figure 10. This model also shows the C=O bonds of the ester groups oriented near parallel to the surface plane. The value of ϕ_{mz} of 67° indicates these bonds are canted, on average, at 23° from the surface plane. Caution must be used in interpreting this angle too quanitatively, however, since the C=O absorption frequencies and line shapes differ somewhat between those calculated and observed (see Figure 5 and Table IV), suggesting that there is some difference in the intermolecular environment of the ester group in the monolayer relative to the bulk crystalline phase.

Summary Conclusions

It has been shown that a variety of substituted disulfide molecules adsorb from solution onto gold surfaces to form densely packed, stable, and oriented monolayer structures. In all cases, the evidence is consistent with the strong attachment of the S–S bond in high density at the gold with the concurrent formation of an ambient-organic interface with the surface properties determined by the other functional groups of the molecules. The detailed structures of the assemblies involve intra- and intermolecular interactions similar to those of the bulk crystalline phases but with a few interesting differences. The ability to produce these model, multifunctional organic overlayers in a specific and controlled way suggests a number of significant applications to interfacial studies in important areas including electrochemistry, adhesion and wetting, biology, microelectronics, and materials science. These possibilities are now being actively pursued in these and other laboratories and will be described in forthcoming papers.

Acknowledgment. The authors gratefully acknowledge many valuable discussions with Professor George Whitesides and Dr. Barry Troughton during the course of this work. The authors also acknowledge David Hwang and Frank Padden for TEM and SEM analyses, respectively, and M. Green for the X-ray diffraction analyses of the gold substrates.

Registry No. DTT-H, 86023-22-5; DTT-F_p, 85977-44-2; DTT-hexadecanoate, 85995-15-9; DTT-PNBA, 85977-45-3; DTT-OAc, 86022-77-7; DTT-TFA, 85977-46-4; HDDS, 1561-75-7; $(HO_2C(CH_2)_2S)_2$, 1119-62-6; $(HO_2C(CH_2)_{10}S)_2$, 23483-56-9; $(H_2N(CH_2)_2S)_2$, 51-85-4; $(CH_3(CH_2)_{17}S)_2$, 2500-88-1; $(CH_3S)_2$, 624-92-0; $(CH_3(CH_2)_3S)_2$, 629-45-8; $(CH_3(CH_2)_7S)_2$, 822-27-5; $(CH_3(CH_2)_9S)_2$, 10496-18-1; $(CH_2CH(CH_2)_{20}S)_2$, 106712-20-3; Au, 7440-57-5.

On the Mechanism of Fe^+-Induced Hydrogen Migrations in Gaseous Octyne/Iron(I) Complexes

Christian Schulze,[†] Helmut Schwarz,*[†] David A. Peake,[‡] and Michael L. Gross*[‡]

Contribution from the Institut für Organische Chemie der Technischen Universität Berlin, D-1000 Berlin 12, West Germany, and the Department of Chemistry, University of Nebraska—Lincoln, Lincoln, Nebraska 68588. *Received November 3, 1986*

Abstract: The study of D-labeled isomeric octynes provides a detailed insight into the gas-phase chemistry of this prototypic hydrocarbon with bare Fe^+. The results not only clearly establish that β-hydrogen transfer is indeed involved in many major decomposition routes, thus providing firm experimental evidence for this often invoked reaction, but also serve as evidence for some unprecedented reactions. Among these reactions is a site-specific 1,2-dehydrogenation of Fe(2-octyne)$^+$, which serves as a further example for "remote functionalization" proceeding via metallacycles. Another of these reactions is the loss of ethylene from the $C_{(1)}/C_{(2)}$ of Fe(4-octyne)$^+$, where, if described in terms of the traditional sequence of oxidative addition/β-hydrogen transfer/reductive elimination, the β-hydrogen transfer to the metal ion is not reversible nor does the reaction constitute the rate-determining step of the overall process. More likely is a process in which a metallacycle is involved. Evidence is presented that the metal ion not only inserts into the activated propargylic C–C bond but also inserts into the homopropargylic, to some extent, and even less activated C–C bonds. Ethylene loss from Fe(4-octyne)$^+$ complexes is associated with an isotope effect of k_H/k_D = 1.1 per deuterium. The rarely observed β-alkyl migrations are not involved in the gas-phase chemistry of Fe(octyne)$^+$ complexes.

The activation of C–H and C–C bonds of hydrocarbons by transition-metal complexes is of fundamental importance in catalysis and has attracted considerable attention.[1] Whereas the direct activation of C–H bonds by an intermolecular process has been observed in solution only recently,[2] the activation of C–C and C–H bonds of hydrocarbons and many functionalized organic compounds by bare metal ions, M^+, in the gas phase has been demonstrated repeatedly during the last decade by using various techniques like ion cyclotron resonance (ICR) mass spectrometry,[3] Fourier transform mass spectrometry (FTMS),[4] ion beam experiments,[5] and collisional activation (CA) mass spectroscopy.[6] From the numerous reports[3-6] of the gas-phase chemistry of transition-metal ions with organic substrates, the sequence involving metal insertion/β-hydrogen shift/competitive ligand loss, suggested for the first time by Allison and Ridge,[3c] is now regarded as a principal route to account for the majority of reductive

Table I. Structures of Products Formed by Fe^+-Induced Rearrangement of Alkenes and Alkynes

	% products		
Fe(alkene)$^+$	**4**	**5**	branching ratio a:b
3-octene	45	55	0.5
4-octene	30	70	0.4
5-decene	35	65	0.5
	% products		
Fe(alkyne)	**9**	**10**	branching ratio a:b
3-heptyne	60	40	1.5
3-octyne	75	25	3.0
4-octyne	60	40	1.5
3-nonyne	65	35	1.9

[†] Berlin.
[‡] Nebraska.

0002-7863/87/1509-2368$01.50/0 © 1987 American Chemical Society